

DISCOVERY OF A YOUNG RADIO PULSAR IN A RELATIVISTIC BINARY ORBIT

V. M. KASPI,^{1,2,3} A. G. LYNE,⁴ R. N. MANCHESTER,⁵ F. CRAWFORD,¹ F. CAMILO,^{4,6} J. F. BELL,⁵ N. D'AMICO,^{7,8}
I. H. STAIRS,⁴ N. P. F. MCKAY,⁴ D. J. MORRIS,⁴ AND A. POSSENTI⁷

Received 2000 February 23; accepted 2000 June 1

ABSTRACT

We report on the discovery of PSR J1141–6545, a radio pulsar in an eccentric, relativistic 5 hr binary orbit. The pulsar shows no evidence of being recycled, having a pulse period $P = 394$ ms, a characteristic age $\tau_c = 1.4 \times 10^6$ yr, and an inferred surface magnetic dipole field strength $B = 1.3 \times 10^{12}$ G. From the mass function and measured rate of periastron advance, we determine the total mass in the system to be $2.300 \pm 0.012 M_\odot$, assuming that the periastron advance is purely relativistic. Under the same assumption we constrain the pulsar's mass to be $M_p \leq 1.348 M_\odot$, and the companion's mass to be $M_c > 0.968 M_\odot$ (both with 99% confidence). Given the total system mass and the distribution of measured neutron star masses, the companion is probably a massive white dwarf that formed prior to the birth of the pulsar. Optical observations can test this hypothesis.

Subject headings: binaries: close — pulsars: general — pulsars: individual (PSR J1141–6545) — relativity — stars: neutron

1. INTRODUCTION

Relativistic binary pulsars have been celebrated as being unique laboratories for high-precision tests of general relativity and accurate determinations of neutron star masses (Taylor & Weisberg 1989; Taylor et al. 1992; Stairs et al. 1998). To date, post-Keplerian general relativistic parameters have been measured for nine binary pulsar systems (see reviews by Taylor et al. 1992; Thorsett & Chakrabarty 1999; Kaspi 1999). Five are double neutron star binaries (PSRs B1913+16, B1534+12, B2127+11C, J1518+4904, and J1811–1736), and four (PSRs J1713+0747, B1802–07, B1855+09, and B2303+46) have white dwarf companions. Through radio timing observations of PSR B1913+16, general relativity has been confirmed at the $\sim 0.3\%$ level (Taylor 1992). Timing observations of these pulsars show that the neutron star masses fall in a narrow range centered on $1.35 M_\odot$ (Thorsett & Chakrabarty 1999). The lack of variation of these masses is surprising given the variety of binary evolution mechanisms by which they were formed.

Of the above relativistic binary systems, all but one are likely to share a similar evolutionary history. The observed pulsar in most of these systems has a large characteristic age τ_c and a low surface magnetic field B relative to the bulk of the isolated pulsar population. This is because the observed neutron star, the firstborn in the binary, was “recycled” by

a phase of mass transfer from its companion as the latter ascended the giant branch (see Bhattacharya & van den Heuvel 1991 for details of neutron star binary evolution). This results in spin-up of the neutron star and the reduction of its magnetic field. The binary observed today has survived the supernova explosion of the secondary (although in the cases of PSRs B2127+11C and B1802–07, which are in globular clusters, the possibility of a more complicated evolutionary history cannot be discounted). The exception among the above binaries is PSR B2303+46, which shows no evidence of having been recycled, having a B and τ_c comparable to the bulk of the isolated pulsar population. PSR B2303+46, long thought to be part of a double neutron star binary, has recently been shown to have a white dwarf companion (van Kerkwijk & Kulkarni 1999) that must have formed prior to the pulsar's birth. Formation mechanisms for such a system have been suggested by Portegies Zwart & Yungelson (1999) and Tauris & Sennels (2000) and involve an initial primary—the white dwarf progenitor—which transferred sufficient matter onto the initial secondary that the latter underwent core collapse.

We report here on PSR J1141–6545, a relativistic binary pulsar recently discovered as part of the Parkes Multibeam Pulsar survey. A preliminary report on this system was presented by Manchester et al. (2000).

2. OBSERVATIONS AND RESULTS

2.1. Discovery Observations

The Parkes multibeam pulsar survey (Lyne et al. 2000), currently underway at the 64 m radio telescope in Parkes, Australia, makes use of a multibeam receiver that operates at a wavelength of 20 cm and permits simultaneous observations of 13 separate regions of the sky (Staveley-Smith et al. 1996). The survey, roughly halfway complete, has been extremely successful, having discovered over 500 new radio pulsars (Camilo et al. 2000; D'Amico et al. 2000). The observing system being used has been described by Lyne et al. (2000). Observations are centered on 1374 MHz, with 288 MHz of bandwidth in each of two orthogonal polarizations for each of the 13 beams. The filtered and amplified signals are fed into a $2 \times 13 \times 96 \times 3$ MHz filter-bank system and are then square law detected. The polarization

¹ Department of Physics and Center for Space Research, Massachusetts Institute of Technology, 70 Vassar Street, Building 37, Cambridge, MA 02139.

² Department of Physics, Rutherford Physics Building, McGill University, 3600 University Street, Montreal, QC, H3A 2T8, Canada.

³ Alfred P. Sloan Research Fellow.

⁴ University of Manchester, Jodrell Bank Observatory, Macclesfield, Cheshire SK11 9DL, England, UK.

⁵ Australia Telescope National Facility, Commonwealth Science and Industrial Research Organization, P.O. Box 76, Epping, NSW 2121, Australia.

⁶ Columbia Astrophysics Laboratory, Columbia University, 550 West 120th Street, New York, NY 10027.

⁷ Osservatorio Astronomico di Bologna, via Ranzani, 1, Bologna, I-40127, Italy.

⁸ Istituto di Radioastronomia del CNR, via Gobetti 101, Bologna, I-40129, Italy.

pairs are summed, and the results are 1 bit digitized every 250 μs and recorded on tape. Observations are of a 35 minute duration. Off-line, the data are dedispersed at many trial dispersion measures (DMs) and subjected to 2^{23} point fast Fourier transforms.

PSR J1141–6545 was discovered in our standard analysis. A periodicity at 394 ms and at $\text{DM} = 118 \text{ pc cm}^{-3}$ were reported as having a signal-to-noise ratio of 15.4 in data obtained on 1999 April 28. Immediately apparent in the discovery observation was the variation in the pulse period because of binary acceleration. Had the pulsar been isolated, its signal-to-noise ratio would have been 40. Confirmation observations were made at Parkes on 1999 July 10. A series of observations in the following week determined the binary parameters.

2.2. Timing Observations

Regular timing observations of PSR J1141–6545 were carried out at numerous epochs from 1999 July 10 through 2000 January 19 using the central beam of the multibeam receiver. In the timing observations the same data acquisition and on-line software system were used as in the regular survey observations. At 1374 MHz we obtained 123 pulse arrival times at a 3 MHz frequency resolution and 31 pulse arrival times using a higher resolution $2 \times 512 \times 0.5$ MHz filter bank. Two observations were made at 600 MHz on 1999 August 23 and 24 using a $2 \times 256 \times 0.125$ MHz filter bank and the standard data acquisition system.

Timing observations were divided into 1 minute sub-integrations that were partially dedispersed into eight subbands and folded at the predicted topocentric pulsar period

using 1024 pulse phase bins. Typical total integration times were ~ 10 minutes. Final dedispersion of the subbands and folding of the subintegrations were done in a subsequent processing step. Each pulse profile was then cross-correlated with a high signal-to-noise template appropriate for the observing frequency and filter-bank resolution. The template for the high-resolution 20 cm observations is shown in Figure 1. The other templates appear similar, including the one at 600 MHz.

The pulse times of arrival (TOAs) that result from the cross-correlation were then subject to a timing analysis using the TEMPO software package,⁹ which converts them to barycentric TOAs at infinite frequency using the Jet Propulsion Laboratory DE200 solar system ephemeris (Standish 1982) and performs a multiparameter least-squares fit for the pulsar spin and binary parameters. During the fitting, the pulsar's position was held fixed at the value determined by interferometric observations (see § 2.3). Also, the DM was determined using the two 600 MHz observations and six 1400 MHz observations obtained on 1999 August 22 and 23, and was held fixed for the rest of the timing analysis.

The results of the timing analysis are presented in Table 1. The fit parameters were P , \dot{P} , the five Keplerian orbital parameters, and a rate of periastron advance $\dot{\omega}$. Upper limits on other post-Keplerian parameters were determined individually. Postfit timing residuals are shown in Figure 2. The uncertainties in the arrival times were determined empirically by demanding that the reduced χ^2 for obser-

⁹ See <http://pulsar.princeton.edu/tempo>.

TABLE 1
MEASURED AND DERIVED PARAMETERS FOR PSR J1141–6545

Parameter	Value
Right ascension ^{a,b} (J2000)	11 ^h 41 ^m 07 ^s .053(15)
Declination ^{a,b} (J2000)	–65°45′18″.85(10)
Galactic longitude ^{a,b}	295°79
Galactic latitude ^{a,b}	–3°86
Dispersion measure ^b , DM (pc cm^{-3})	116.017(11)
Flux density ^a at 1384 MHz (mJy)	3.3(5)
Flux density ^a at 2496 MHz (mJy)	0.9(5)
Pulse FWHM at 20 cm	0.011 P
Rotation measure, RM (rad m^{-2})	–86(3)
Period, P (s)	0.3938978339002(22)
Period derivative, \dot{P}	$4.3070(2) \times 10^{-15}$
Epoch (MJD ^c)	51369.8525
Orbital period, P_b (days)	0.197650965(5)
Eccentricity, e	0.171881(9)
Projected semimajor axis, $a \sin i \equiv x$ (lt-s)	1.85945(1)
Longitude of periastron, ω	42°436(5)
Epoch of periastron, T_0 (MJD ^c)	51369.854549(3)
Advance of periastron, $\dot{\omega}$ (deg yr^{-1})	5.33(2)
Relativistic time dilation and gravitational redshift, γ (ms)	< 2.5 (3σ)
Orbital period derivative, $ \dot{P}_b $	$< 5 \times 10^{-11}$ (3σ)
Rate of change of $a \sin i$, $ \dot{x} $ (lt-s s^{-1})	$< 5 \times 10^{-12}$ (3σ)
Characteristic age, τ_c (Myr)	1.4
Inferred surface dipole magnetic field strength, B (G)	1.3×10^{12}
Spin-down luminosity, \dot{E} (ergs s^{-1})	6.9×10^{32}
Mass function, (M_\odot)	0.176701(3)
Total system mass, M (M_\odot)	2.300(12)

NOTE.—Numbers in parentheses represent 1σ uncertainties in the last digit quoted.

^a Parameter determined from ATCA observations. See § 2.3.

^b Parameter determined at a single epoch and held fixed in timing analysis. See § 2.2.

^c Modified Julian Day $\text{MJD} = \text{JD} - 2,400,000.5$.

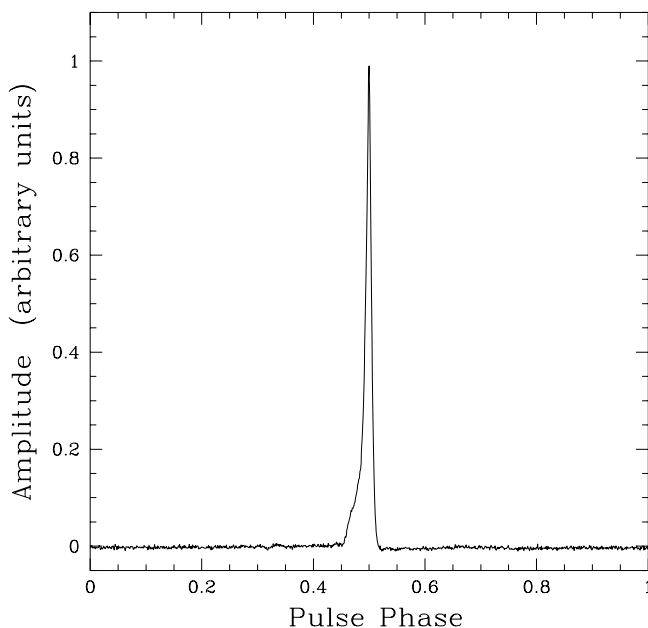


FIG. 1.—Average pulse profile for PSR J1141–6545 at 20 cm, obtained with 500 kHz frequency resolution. The pulse period is 394 ms. The effective dispersion smearing is 0.19 ms or $(4.8 \times 10^{-4})P$.

variations over a short span (1–2 days) be unity. The formal reduced χ^2 for these residuals is 4.7 (145 degrees of freedom). This clearly indicates that there are unmodeled effects in the data. That the residuals as a function of orbital phase do not display systematic trends leads us to believe that the orbital parameters are not biased by these effects. Indeed, the two arrival times with the largest residuals, near epoch 1999.96, are at orbital phases separated by ~ 0.5 . The unmodeled features may be manifestations of standard “timing noise,” a stochastic process seen in many young pulsars like PSR J1141–6545 (e.g., Arzoumanian et al. 1994). This may bias the measured spin parameters slightly.

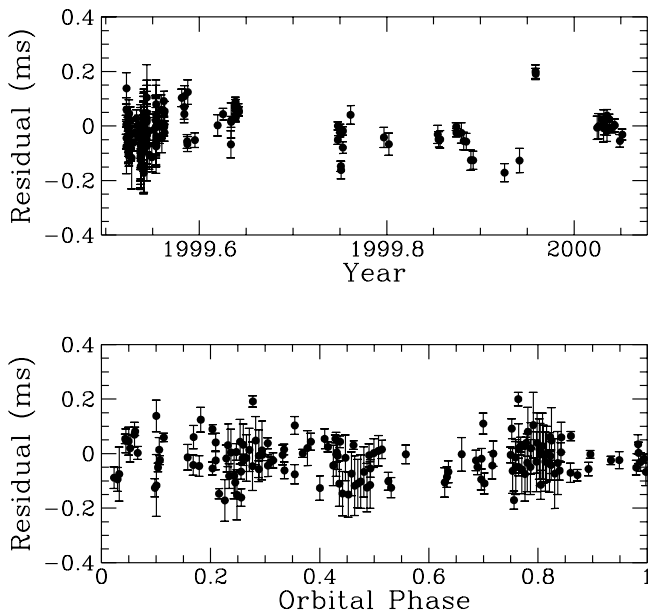


FIG. 2.—Timing residuals for PSR J1141–6545. *Top panel*: residuals as a function of time. *Bottom panel*: residuals as a function of orbital phase, where phase 0/1 is periastron. The RMS timing residual is 66 μ s or $(1.7 \times 10^{-4})P$.

2.3. Radio Interferometric Observations

PSR J1141–6545 was observed on 1999 August 22 and 23 with the Australia Telescope Compact Array (ATCA), which is located in Narrabri, Australia. The array was in its 6D configuration, which has a maximum baseline of 5878 m. The observations were done simultaneously in pulsar gating mode at center frequencies of 1384 and 2496 MHz, with 128 MHz of bandwidth in each of two linear polarizations for each frequency. The primary and secondary calibrators for the observations were the bright radio point sources 1934–638 and 1329–665. The data were processed using the MIRIAD processing package.¹⁰ After standard interference flagging and calibration were done, on- and off-pulse images were formed. The off-pulse emission was then subtracted from the UV data set, leaving only on-pulse emission from the pulsar. A point source was then fitted to these UV data using the nominal position and a rough estimate of the flux density of the pulsar. A model of the resulting UV data was then fitted using trial positions and flux densities for the pulsar by means of the MIRIAD UVFIT task. Best-fit values and uncertainties were obtained for both the 1384 and 2496 MHz data sets. Since the pulsar is brighter at 1384 MHz, we use the more accurate fitted position from that data set in the timing analysis (see Table 1). The 1384 MHz pulsed flux (~ 3.3 mJy) is consistent with that estimated from the Parkes observations; the 3σ upper limit on pointlike radio emission off pulse is 0.66 mJy at this frequency.

2.4. Polarization

We have measured the polarization properties of PSR J1141–6545, which are especially interesting given the possibility of significant precession of the pulsar (see § 3.3 below). Observations were made on 2000 March 26 (MJD 51,629) using the center beam of the multibeam receiver and the Caltech correlator (Navarro 1994). Instrumental phases and gains were calibrated using a pulsed-noise signal injected at 45° to the two signal probes (see Navarro et al. 1997 for a full description). Two 25 minute observations using 64 MHz bandwidth at orthogonal feed angles were summed to produce the polarization profiles shown in Figure 3. Position angles were corrected for Faraday rotation in the Earth’s ionosphere. The ionospheric contribution to the rotation measure (RM) was estimated to be -3.2 rad m^{-2} at the time of the observation by using an ionospheric model, so the plotted angles are approximately 9° greater than those observed. The precision of the absolute position angles is limited by the uncertainty in this correction, which we estimate to be $\pm 2^\circ$.

On average, the pulse profile is 16% linearly polarized (see Fig. 3). The position angle shows a complicated variation across the pulse with a clear orthogonal transition in the leading wing and a sharp drop toward the trailing edge of the pulse. The circular polarization is relatively strong, with a mean value of -10% . There is a possible reversal in the sign of V at a pulse phase slightly preceding the orthogonal transition in the linear polarization. These properties are not consistent with any simple model for the polarization. The shape of the total intensity profile suggests that the main peak is near the trailing edge of a conal beam. This may be supported by the location of the reversal of sign of V , which is usually (but not always) located near the center

¹⁰ See <http://www.atnf.csiro.au/computing/software/miriad/>.

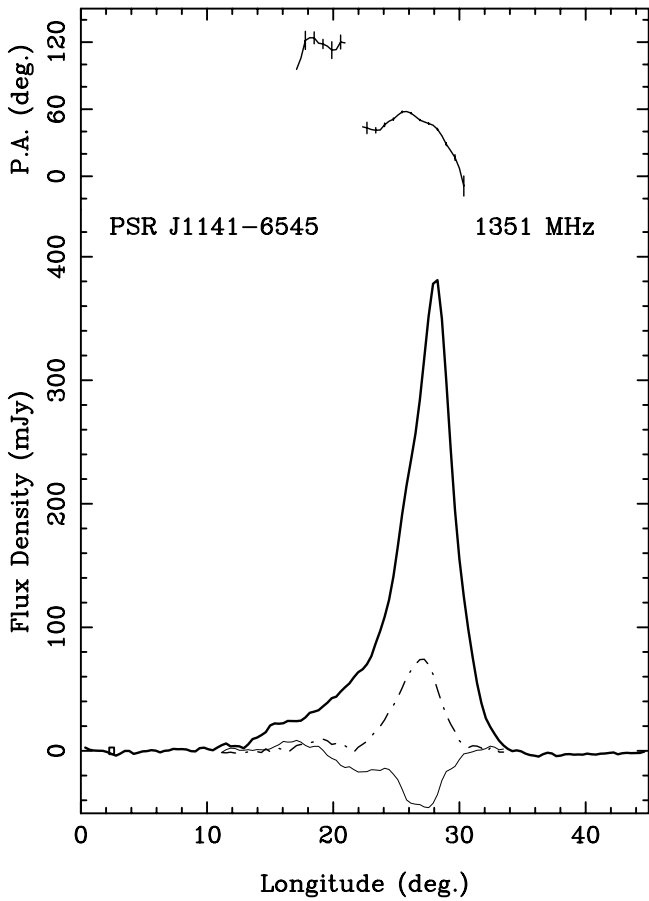


FIG. 3.—Polarization parameters for PSR J1141–6545 at 1351 MHz. In the lower part of the figure the pulse total intensity (Stokes I) is given by the thick line, the linearly polarized intensity [$L = (Q^2 + U^2)^{1/2}$] by the dash-dotted line, and the circularly polarized intensity (Stokes V) by the thin line. V is defined in the sense that the left-circular polarization (IEEE convention) is positive. The upper part of the figure gives the position angle above the Earth's ionosphere, measured from north toward east, of the linearly polarized component.

of the beam (Han et al. 1998). However, the observed position angle variation is certainly not consistent with a rotating vector model having a beam center on the leading wing.

The interstellar component of the RM, estimated by computing the weighted mean position angle difference between the two halves of the observed band, is $-86 \pm 3 \text{ rad m}^{-2}$. This implies a mean line-of-sight interstellar field, weighted by the electron density along the path, of $0.9 \mu\text{G}$ directed away from us. RMs of neighboring pulsars are of mixed sign and magnitude (Han, Manchester, & Qiao 1999). At the estimated distance of 3.2 kpc, as inferred from the DM and a model for the Galactic electron distribution (Taylor & Cordes 1993), the path to the pulsar crosses the Carina arm; the structure of the Galactic magnetic field in this region is evidently complex.

3. DISCUSSION

PSR J1141–6545 is different from most of the other known relativistic binary pulsars in several important respects. The pulsar's characteristic age, $\tau_c = 1.4 \times 10^6 \text{ yr}$, and inferred surface magnetic field strength, $B = 1.3 \times 10^{12} \text{ G}$, are similar to those of the bulk of the isolated pulsar population. Thus, PSR J1141–6545 is unlikely to have ever been recycled. Like the other short P_b , eccentric relativistic binaries, it may be a double neutron star binary, but if so,

we must be observing the second-formed neutron star in its short-lived radio pulsar phase. In this case, its companion could still be an observable radio pulsar that was not detected in our Parkes observations, either because its short spin period varies too rapidly because of the binary orbit (a possibility we are checking, given our knowledge of the binary orbit) or because its radio beam does not intersect our line of sight.

However, we show here that the companion is unlikely to be a second neutron star, given the system's mass function, its rate of precession $\dot{\omega}$, and what is known about the neutron star mass distribution. The mass function is given by

$$f(M_p) = \frac{4\pi^2(a \sin i)^3}{GP_b^2} = \frac{M_c^3 \sin^3 i}{(M_p + M_c)^2}, \quad (1)$$

where M_p and M_c are the pulsar and companion masses, respectively, P_b is the orbital period, and $a \sin i$ is the projected semimajor axis of the pulsar orbit. This provides a constraint on the minimum M_c for any assumed M_p by setting i , the inclination of the orbital angular momentum with respect to the line of sight, to 90° . In addition, $\dot{\omega}$, under the assumption that it is due to general relativistic periastron precession (but see § 3.2), is given by

$$\dot{\omega}_{\text{GR}} = 3 \left(\frac{P_b}{2\pi} \right)^{-5/3} (T_\odot M)^{2/3} (1 - e^2)^{-1}, \quad (2)$$

where $T_\odot = 4.925490947 \times 10^{-6} \text{ s}$. This then determines the total system mass $M = M_p + M_c$. For $\dot{\omega} = (5^\circ 32 \pm 0^\circ 02) \text{ yr}^{-1}$ (Table 1), $M = 2.300 \pm 0.012 M_\odot$. Figure 4 shows these constraints in the M_p - M_c phase space. The shaded region is ruled out by the mass function. The intersection of the $\dot{\omega}$ straight line with the boundary of this region determines the maximum allowed pulsar mass:

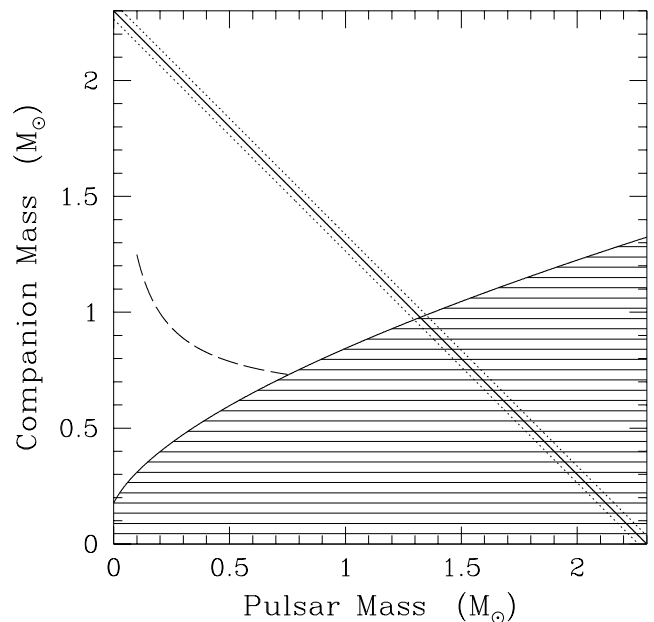


FIG. 4.—Allowed companion mass (M_c) and pulsar mass (M_p) phase space. The shaded area is ruled out by the mass function. The solid straight line shows the constraint on the total mass M implied by $\dot{\omega}$, assuming it is purely relativistic. The dotted lines representing the 3σ uncertainties. The dashed line shows allowed masses for a non- or slowly rotating helium star companion, under the assumption that the observed $\dot{\omega}$ is partially due to a tide raised by the neutron star (see § 3.2).

$M_p < 1.331 M_\odot$ (1 σ) or $M_p < 1.348 M_\odot$ (3 σ). Similarly, we set a lower limit $M_c > 0.974 M_\odot$ (1 σ) or $M_c > 0.968 M_\odot$ (3 σ).

Thorsett & Chakrabarty (1999) showed that measurements of neutron star masses are consistent with all being drawn from a Gaussian distribution that have a mean and standard deviation of 1.35 and 0.04 M_\odot , respectively. The parameters in the PSR J1141–6545 system are thus interesting; if M_p is close to its maximum allowed value corresponding to $i \simeq 90^\circ$, as would be consistent with other neutron star masses, then its companion has mass much lower than those of all known neutron stars, and therefore is unlikely to be one. Of course on a posteriori statistical grounds, $i \simeq 90^\circ$ is improbable. On the other hand, a smaller i implies a less massive pulsar. For the median value $i = 60^\circ$, $M_p = 1.17 M_\odot$, and $M_c = 1.13 M_\odot$, both significantly lower than for any other known neutron stars. Note that none of these values can be ruled out based on neutron star stability arguments, since masses of as little as $\sim 0.1 M_\odot$ are allowed (e.g., Colpi, Shapiro, & Teukolsky 1993). However the formation mechanism for such low-mass neutron stars is unclear.

3.1. A Neutron Star/White Dwarf Binary?

A more likely possibility is that the PSR J1141–6545 system is a neutron star/CO white dwarf binary seen edge-on. (ONeMg white dwarfs have a minimum mass of $\sim 1.1 M_\odot$ [Wanajo, Hashimoto, & Nomoto 1999], so this possibility cannot be ruled out.) The evolutionary history of the PSR J1141–6545 binary, if the companion is a massive white dwarf, is then clear (see, e.g., Dewey & Cordes 1987; Portegies Zwart & Yungelson 1999; Tauris & Sennels 2000): the system originated as a binary consisting of two main-sequence stars having mass ratio near unity but with neither sufficiently massive to independently form a neutron star. For example, the primary may have had a mass of 7 M_\odot and the secondary 5 M_\odot . The primary evolved first to form the white dwarf, in the process transferring sufficient matter onto the secondary for its mass to exceed that necessary to form a neutron star. After the white dwarf formed it spiraled into the envelope of the now more massive secondary as the latter ascended the giant branch, greatly decreasing the orbital period, and ejecting the common envelope. The secondary, a helium star after the ejection of the envelope, then exploded into a supernova, which fortuitously did not disrupt the binary. The radio pulsar we see is therefore the second evolved star.

The evolutionary scenario in which a massive white dwarf forms prior to the neutron star has been considered in population synthesis studies. Dewey & Cordes (1987) and Portegies Zwart & Yungelson (1999) showed that the birth-rate of white dwarf/young pulsar binaries is comparable to that of double neutron star binaries. However, Portegies Zwart & Yungelson (1999) argued that the white dwarf should have a mass of $\gtrsim 1.1 M_\odot$, a result of their assumption that a neutron star forming binary had to have an initial primary mass of more than 7 M_\odot . To form a $\sim 1 M_\odot$ white dwarf, an initial minimum primary mass of $\sim 6 M_\odot$ is required (S. Portegies Zwart 2000, private communication). The work of Tauris & Sennels (2000) confirms that white dwarf/young neutron star systems should be observable, but they suggest that the birthrate of such systems is much higher than that of double neutron star systems. A lower allowed initial primary mass for forming white dwarfs in the

Portegies Zwart & Yungelson (1999) analysis could reduce the disagreement.

One prediction of the binary evolution theory is that the space velocity of PSR J1141–6545 will not be greater than $\sim 150 \text{ km s}^{-1}$ (Dewey & Cordes 1987; Tauris & Sennels 2000). At a distance of 3.2 kpc, this implies a proper motion of $\sim 10 \text{ mas yr}^{-1}$, which may be measurable by timing on a timescale of a few years. VLBI observations may also be able to detect it. However, given the pulsar's timing age, Galactic latitude, and distance estimate and assuming that the pulsar was born in the Galactic plane, the component of the pulsar's space velocity perpendicular to the plane must be $\sim 150(d/3.2 \text{ kpc}) \text{ km s}^{-1}$, already large compared to the predictions.

If the companion is indeed a white dwarf, allowing for interstellar reddening, its B magnitude is likely to be in the range 25–26.5 and R in the range 24.5–26. From a Digital Sky Survey image of the field, it is clear that the field is relatively crowded, but not impossibly so. Excellent seeing conditions on the VLT would allow detection of the companion. If detected, then a follow-up temperature measurement using the *HST* may provide a useful age constraint.

3.2. Classical Contribution to $\dot{\omega}$?

The observed $\dot{\omega}$ may not be purely relativistic, in which case the above conclusions would have to be modified. Classical contributions to $\dot{\omega}$ can come either from tidal deformation of the companion by the neutron star (significant only if the companion is nondegenerate) or from a rotation-induced quadrupole moment in the companion, possibly relevant if it is a rapidly rotating white dwarf. We consider these possibilities in turn.

A tide raised on the companion star gives it a quadrupole moment that results in a classical apsidal advance, $\dot{\omega}_{\text{tide}}$, given by

$$\dot{\omega}_{\text{tide}} = 3.44 \times 10^6 k_2 \left(\frac{M_p}{M_c} \right) \left(\frac{M}{M_\odot} \right)^{-5/3} \left(\frac{R_c}{R_\odot} \right)^5 \text{ deg yr}^{-1}, \quad (3)$$

where R_c is the companion radius and k_2 its apsidal constant, a measure of its internal density distribution (Roberts, Masters, & Arnett 1976; Smarr & Blandford 1976). A hydrogen main-sequence star companion could in principle fit in the orbit, but would result in a classical $\dot{\omega}$ of ~ 1000 times the relativistic value (see Masters & Roberts 1975), so it is certainly ruled out. However, a helium main-sequence star has a much smaller radius and would result in a classical $\dot{\omega}$ that is comparable to the expected relativistic value. We have explored this possibility by considering a range of values for M_p and M_c and finding the expected $\dot{\omega} = \dot{\omega}_{\text{tide}} + \dot{\omega}_{\text{GR}}$ that match the observed value. For these calculations, we assumed $k_2(R_c/R_\odot)^5 = 4 \times 10^{-6}(M_c/M_\odot)^{4.59}$, as derived by Roberts et al. (1976). In Figure 4 the dashed line shows the allowed locus in the M_p - M_c space for a non or slowly rotating helium star companion. Clearly, this is possible only if $M_p \leq 0.75 M_\odot$. This seems unlikely given observed masses of other neutron stars.

A rapidly rotating white dwarf would have a quadrupole moment that could result in a significant classical $\dot{\omega}$ (Roberts et al. 1976; Smarr & Blandford 1976). However, unlike the tidal quadrupole, the rotationally induced quadrupole lies in a plane perpendicular to the white dwarf spin axis. Since the pulsar formed after the white dwarf, it is

unlikely that the white dwarf spin axis is aligned with the orbital angular momentum, since this would demand a fortuitously symmetric supernova explosion. A misalignment of the angular momenta results in classical spin-orbit coupling, that is, a precession of the orbital plane di/dt as in the pulsar/B-star binary PSR J0045–7319 (Lai, Bildsten, & Kaspi 1995; Kaspi et al. 1996). This precession would manifest itself as a time-variable projected semimajor axis $x \equiv a \sin i$. In general, the magnitude of di/dt is comparable to that of the periastron precession $\dot{\omega}$ (Wex 1998). For PSR J1141–6545, we find an upper limit on \dot{x} that is much smaller than $\dot{\omega}$ (Table 1). This might suggest that spin-orbit coupling is unlikely to be occurring. However, \dot{x} varies as $\cos i$; since $i \simeq 90^\circ$ (especially if $\dot{\omega}_{\text{GR}}$ is smaller than our observed value), we cannot rule out orbital plane precession, i.e. a large di/dt .

The above reasoning also holds for a helium-star companion that is rotating rapidly. In this case, the dashed line in Figure 4 is inappropriate, since it assumes no contribution from a rotation-induced quadrupole moment. Hence, we cannot presently rule out this possibility. However, a $1 M_\odot$ helium main-sequence star would be considerably brighter than a white dwarf; assuming that it is on the helium main sequence, it would have bolometric luminosity $\log(L/L_\odot) = 2.4$ and $T_{\text{eff}} = 50,000$ K (Kippenhahn & Weigert 1990). Using bolometric corrections from Bessell, Castelli, & Plez (1998) and given the distance and expected reddening, a helium star should have $B \simeq 17$ and should be easily distinguishable from a white dwarf.

3.3. Future Relativistic Observables

The prospects for a high-precision determination of both of the component masses in the PSR J1141–6545 binary system are excellent. Our upper limit on the combined time dilation and gravitational redshift parameter γ is shown in Table 1. Note that this is largely independent of which model for the system is correct. Given that the fractional uncertainty in γ scales as $T^{-3/2}$, where T is the observing span (Damour & Taylor 1992), we expect a 3σ detection by 2001, assuming $\dot{\omega}$ is purely relativistic (for which $\gamma \simeq 0.7$ ms for $M_p = 1.32 M_\odot$). Furthermore, a general relativistic orbital period derivative, \dot{P}_b , should be measurable with interesting precision by 2004, given that its fractional uncertainty scales as $T^{-5/2}$, and its expected value is -3.5×10^{-13} . Thus, continued high-precision timing observations of PSR J1141–6545 will eventually test our assumptions about a purely relativistic $\dot{\omega}$. Although the orbit is likely to be highly inclined, measurement of the Shapiro delay will be difficult; the maximum expected delay is only $\sim 5 \mu\text{s}$, well below our current timing precision.

Although PSR J1141–6545 will coalesce in ~ 1.5 Gyr because of gravitational-radiation-induced orbit decay, it,

and coalescing neutron star/white dwarf binaries in general, will not be detected by the Laser Interferometer Gravitational-Wave Observatory (LIGO). The detectability depends on the frequency of the emitted radiation near the time of coalescence. This depends on the size of the orbit at coalescence, which, to order of magnitude, is the white dwarf radius, $\sim 10^9$ cm. This implies an orbital frequency of ~ 0.1 Hz at coalescence; the implied gravitational wave frequency, twice the orbital frequency, is well outside the LIGO band of 10–10,000 Hz. However, such signals would be within the 0.00001–1 Hz band of the proposed Laser Interferometric Space Antenna (Bender 1998).

General relativistic geodetic precession (Barker & O’Connell 1975) is predicted to result in the precession of the pulsar’s spin axis at a rate of $\sim 1:35 \text{ yr}^{-1}$ (assuming a purely relativistic $\dot{\omega}$ for $i = 90^\circ$). This is greater than that predicted for the two pulsars for which it has been observed, PSR B1913+16 (Weisberg, Romani, & Taylor 1989; Kramer 1998) and PSR B1534+12 (Arzoumanian 1995; Stairs et al. 2000), although the measured amplitude will be suppressed by a possibly large factor that depends on the unknown line-of-sight geometry and spin-orbit misalignment. Given the narrow pulse profile seen in PSR J1141–6545 (Fig. 1, FWHM of $0.011P$), this effect could be detected in a few years, barring unfortunate geometries. Thus far, we have detected no strong evidence for pulse profile changes, although a detailed analysis is beyond the scope of this paper.

That the pulsar was not detected in past pulsar radio surveys of the region is intriguing. The Johnston et al. (1992) 20 cm survey of the Galactic plane had a minimum detectable flux density of ~ 1 mJy, below the pulsar’s 20 cm flux density of 3.3 mJy. At this frequency the pulsar displays no evidence for scintillation. The Parkes all-sky survey at 70 cm also may have been able to detect it. That survey’s sensitivity reached 20 mJy for the Galactic plane sources; extrapolating the flux densities in Table 1, the estimated flux density at 70 cm is ~ 40 mJy. Scattering for the pulsar at that frequency is negligible. Thus, it is plausible that the pulsar’s beam has only recently precessed into our line of sight, a result of geodetic precession. If so, the pulse profile should be evolving rapidly.

The Parkes radio telescope is part of the Australia Telescope, which is funded by the Commonwealth of Australia for operation as a National Facility managed by CSIRO. We thank M. Kramer for assistance at Parkes, B. Gaensler for help with the ATCA data, and V. Kalogera, M. van Kerkwijk, S. Portegies Zwart, F. Rasio and S. Thorsett for helpful discussions. V. M. K. is supported by a National Science Foundation CAREER award (AST 98-75897). F. C. is supported by NASA grant NAG 5-3229.

REFERENCES

- Arzoumanian, Z. 1995, Ph.D. thesis, Princeton Univ.
 Arzoumanian, Z., Nice, D. J., Taylor, J. H., & Thorsett, S. E. 1994, *ApJ*, 422, 671
 Barker, B. M. & O’Connell, R. F. 1975, *ApJ*, 199, L25
 Bender, P. L. 1998, *BAAS*, 193, 48.03
 Bessell, M. S., Castelli, F. & Plez, B. 1998, *A&A*, 333, 231
 Bhattacharya, D. & van den Heuvel, E. P. J. 1991, *Phys. Rep.*, 203, 1
 Camilo, F., et al. 2000, in *IAU Colloq. 177, Pulsar Astronomy: 2000 and Beyond*, ed. M. Kramer, N. Wex, & R. Wielebinski (San Francisco: ASP), 3
 Colpi, M., Shapiro, S. L., & Teukolsky, S. A. 1993, *ApJ*, 414, 717
 D’Amico, N. et al. 2000, *Astrophys. Lett. and Commun.*, in press
 Damour, T., & Taylor, J. H. 1992, *Phys. Rev. D*, 45, 1840
 Dewey, R. J., & Cordes, J. M. 1987, *ApJ*, 321, 780
 Han, J. L., Manchester, R. N., & Qiao, G. J. 1999, *MNRAS*, 306, 371
 Han, J. L., Manchester, R. N., Xu, R. X., & Qiao, G. J. 1998, *MNRAS*, 300, 373
 Johnston, S., Lyne, A. G., Manchester, R. N., Kniffen, D. A., D’Amico, N., Lim, J., & Ashworth, M. 1992, *MNRAS*, 255, 401
 Kaspi, V. M. 1999, in *General Relativity and Relativistic Astrophysics*, ed. C. P. Burgess & R. C. Myers (San Francisco: ASP), 3
 Kaspi, V. M., Bailes, M., Manchester, R. N., Stappers, B. W., & Bell, J. F. 1996, *Nature*, 381, 584
 Kippenhahn, R. & Weigert, A. 1990, *Stellar Structure and Evolution* (Heidelberg: Springer)
 Kramer, M. 1998, *ApJ*, 509, 856

- Lai, D., Bildsten, L., & Kaspi, V. M. 1995, *ApJ*, 452, 819
Lyne, A. G., et al. 2000, *MNRAS*, 312, 698
Manchester, R. N., et al. 2000, in *IAU Colloq. 177, Pulsar Astronomy: 2000 and Beyond*, ed. M. Kramer, N. Wex, & R. Wielebinski (San Francisco: ASP), 49
Masters, A. R., & Roberts, D. H. 1975, *ApJ*, 195, L107
Navarro, J. 1994 Ph.D. thesis, California Institute of Technology
Navarro, J., Manchester, R. N., Sandhu, J. S., Kulkarni, S. R., & Baile, M. 1997, *ApJ*, 486, 1019
Portegies Zwart, S. F., & Yungelson, L. R. 1999, *MNRAS*, 309, 26
Roberts, D. H., Masters, A. R., & Arnett, W. D. 1976, *ApJ*, 203, 196
Smarr, L. L., & Blandford, R. 1976, *ApJ*, 207, 574
Stairs, I. H., Arzoumanian, Z., Camilo, F., Lyne, A. G., Nice, D. J., Taylor, J. H., Thorsett, S. E., & Wolszczan, A. 1998, *ApJ*, 505, 352
Stairs, I. H., Thorsett, S. E., Taylor, J. H., & Arzoumanian, Z. 2000, in *IAU Colloq. 177, Pulsar Astronomy: 2000 and Beyond*, ed. M. Kramer, N. Wex, & R. Wielebinski (San Francisco: ASP), 121
Standish, E. M. 1982, *A&A*, 114, 297
Staveley-Smith, L., et al. 1996, *Publ. Astron. Soc. Australia*, 13, 243
Tauris, T. M., & Sennels, T. 2000, *A&A*, 355, 236
Taylor, J. H. 1992, *Philos. Trans. R. Soc. London A*, 341, 117
Taylor, J. H., & Cordes, J. M. 1993, *ApJ*, 411, 674
Taylor, J. H., & Weisberg, J. M. 1989, *ApJ*, 345, 434
Taylor, J. H., Wolszczan, A., Damour, T., & Weisberg, J. M. 1992, *Nature*, 355, 132
Thorsett, S. E., & Chakrabarty, D. 1999, *ApJ*, 512, 288
van Kerkwijk, M., & Kulkarni, S. R. 1999, *ApJ*, 516, L25
Wanajo, S., Hashimoto, M. A., & Nomoto, K. 1999, *ApJ*, 523, 409
Weisberg, J. M., Romani, R. W., & Taylor, J. H. 1989, *ApJ*, 347, 1030
Wex, N. 1998, *MNRAS*, 298, 997